ACS SENSORS

pubs.acs.org/acssensors

Article

Engineered Sensor Zebrafish for Fast Detection and Real-Time Tracking of Apoptosis at Single-Cell Resolution in Live Animals

Hao Jia, Yanlong Song, Bin Huang, Wei Ge, and Kathy Qian Luo*

Cite This: *ACS Sens.* 2020, 5, 823−830

Read Online

ACCESS | Metrics & More | Article Recommendations | Supporting Information

ABSTRACT: Apoptosis plays crucial roles during development and in disease conditions. While there are some methods to detect apoptosis in vitro, most of them are end-point assays that cannot be used to detect apoptosis in the physiological context of live animals. In this study, transgenic sensor zebrafish were generated that specifically produce a fluorescence resonance energy transfer (FRET)-based biosensor in the zebrafish skin. Under normal conditions, the skin cells of the sensor zebrafish emit green fluorescence; when caspase-3 is activated during apoptosis, the skin cells of the sensor zebrafish switch to emitting blue fluorescence. Through time-lapse FRET imaging with the sensor zebrafish, we observed that caspase-3 can be activated within 5 min and apoptosis can be completed in around 30 min in live zebrafish, no matter the apoptosis occurs several hours after UV irradiation or during the normal development. Using the sensor zebrafish, we found that apoptosis can occur in different parts of the zebrafish skin including the skin covering the trunk, eye, yolk sac, and head during development. Interestingly, we observed that the yolk sac diameter of the zebrafish reduced from 723.8 ± 25.1 μm at 24 h postfertilization (hpf) to 346.1 ± 24.6 μm at 120 hpf. To accommodate this dramatic reduction of the yolk sac size, we found that some excess skin cells on the surface of the yolk sac were removed by apoptosis during this process. The sensor zebrafish provide a powerful and convenient tool for the noninvasive and real-time detection of apoptosis at the single-cell resolution in live zebrafish.

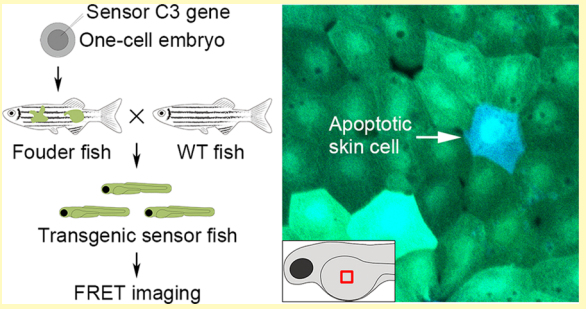

KEYWORDS: *apoptosis, caspase-3, FRET, real-time, in vivo imaging, skin development, zebrafish*

Apoptosis plays important roles during organ formation and in the maintenance of tissue homeostasis by removing excess cells.[1] Malfunction of apoptosis is closely related to the development of many important diseases, including cancer,[2] autoimmune diseases,[3] diabetes,[4] and neurodegenerative diseases.[5] Both extrinsic and intrinsic pathways of apoptosis converge on the activation of caspases, especially, caspase-3.[6] Activated caspases specifically cleave a set of intracellular substrates such as cytokeratins, poly(ADP-ribose) polymerase (PARP), and the nuclear protein NuMA to execute apoptosis.[7] Apoptosis is a fast, asynchronous, and spatiotemporal process occurring in live animals.[8] Some methods have been developed to detect apoptosis in cells and tissue sections such as terminal deoxynucleotidyl transferase dUTP nick end labeling (TUNEL) assay[9] and annexin V staining.[10] These conventional methods require complicated experimental steps and cannot be used to detect apoptosis in real-time and in the physiological context of live animals.

Some attempts have been made to detect apoptosis in several in vivo model systems. For example, several probes have been designed to detect apoptosis in the live embryos or pupae of *Drosophila*, but the low resolution and the narrow detection window limited their applications.[8,11,12] Compared with *Drosophila*, zebrafish represent a vertebrate animal model and have a transparent body that is beneficial for in vivo imaging.[13] An annexin V reporter and a caspase-3 reporter were used for generating transgenic zebrafish to detect apoptosis in embryos, but the signal-to-noise ratio was low.[14,15] Two fluorogenic caspase reporters were used to visualize apoptosis occurring in zebrafish embryos by microinjecting the reporters' mRNA, but their resolution is not high. Besides, these two reporters were encoded by two recombinant genes, thus introducing both of them into the genome of transgenic zebrafish is rather challenging.[16,17]

In this study, we wanted to overcome the limitations of apoptosis detection in live animals, that is, to achieve noninvasive and real-time tracking of apoptosis at single-cell resolution. To achieve this goal, we chose zebrafish as the model animal. We generated transgenic sensor zebrafish that express an in-house-developed fluorescence resonance energy transfer (FRET)-based caspase biosensor (sensor C3)[18] in zebrafish skin. Due to the high FRET effect produced by

Received: December 16, 2019
Accepted: February 24, 2020
Published: February 24, 2020

https://dx.doi.org/10.1021/acssensors.9b02489
ACS Sens. 2020, 5, 823−830

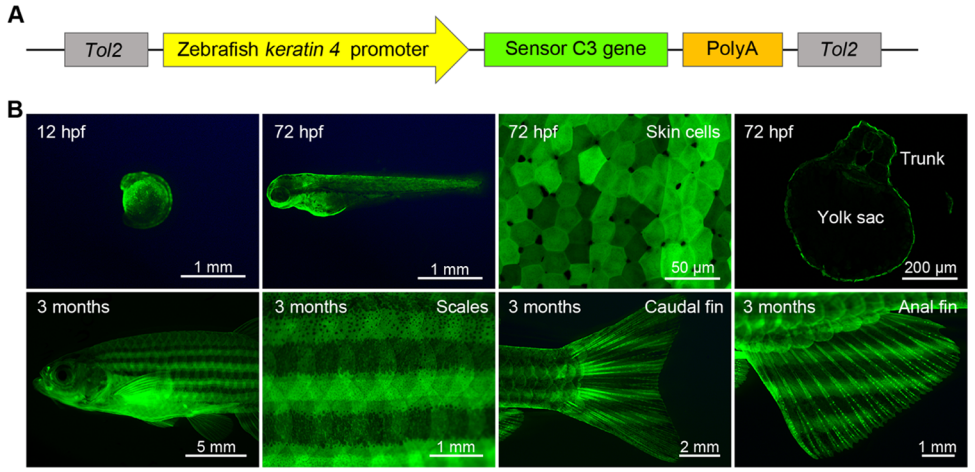

Figure 1. Generation and expression profile of the transgenic sensor zebrafish. (A) Schematic diagram showing the major components of the *Tol2* transposon construct that was used to generate transgenic sensor zebrafish. (B) Sensor C3 was expressed under a zebrafish *krt4* promoter, and its expression pattern was examined in live Tg(*krt4*:sensor C3) zebrafish at different developmental stages and in different regions. The high-magnification image of individual skin cells from 72 hpf zebrafish was taken from live zebrafish using a 514 nm laser. The upper right 72 hpf image was obtained after immunostaining of a fixed zebrafish section with an anti-GFP antibody using a 488 nm laser, which shows that sensor C3 was expressed in the outermost single layer of the zebrafish larvae skin cells. Other images were taken using a GFP filter from live zebrafish.

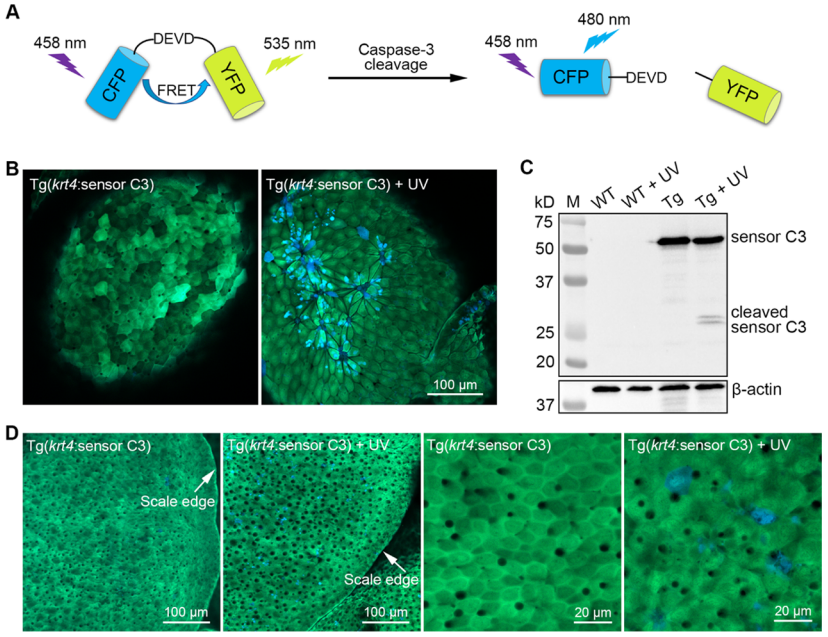

Figure 2. Principle and validation of sensor C3 in detecting apoptosis in sensor zebrafish. (A) Design and principle of sensor C3 in detecting apoptosis. (B) Tg(*krt4*:sensor C3) zebrafish larvae (72 hpf) were irradiated twice with UV at a dosage of 200 mJ/cm^2. Four hours later, FRET imaging revealed apoptotic skin cells in the yolk sac region. The green cells are nonapoptotic cells, and the blue cells are apoptotic cells. (C) Results from the Western blotting show that the full-length sensor C3 proteins were expressed in the Tg(*krt4*:sensor C3) zebrafish larvae, and some censor 3 proteins were cleaved into CFP and YFP after UV irradiation. The Western blotting experiments were performed twice, which produced similar results. (D) Blue apoptotic cells were detected in the skin (on top of the scales) of the Tg(*krt4*:sensor C3) adult zebrafish 4 h after UV irradiation. Single apoptotic cells can be clearly visualized at higher magnification (right two images).

sensor C3,[18−20] we could easily observe zebrafish sensor cells change their fluorescence from green to blue when undergoing apoptosis at single-cell resolution in live zebrafish embryos and adults without postacquisition procedures. As the sensor C3 proteins can be produced in zebrafish cells and FRET imaging is a noninvasive observation method, we were able to track apoptotic cells within the same zebrafish in real-time, and the spatiotemporal tracking lasted for at least 5 days. With these sensor zebrafish, we discovered a new role of apoptosis in removing excess skin cells during zebrafish development.

EXPERIMENTAL SECTION

Zebrafish Husbandry. The wide-type (WT) zebrafish of the AB strain were used in this study to generate sensor zebrafish. Zebrafish were maintained in the ZebTEC system (28 ± 1 °C; photoperiod of 14 h light to 10 h dark). All of the experiments were approved by the panel of the University of Macau Animal Research Ethics.

Generation of Transgenic Sensor Zebrafish. The adult zebrafish genome was extracted with the DNeasy Blood & Tissue Kit (Qiagen). A 2.2 kb skin-specific *keratin 4* (*krt4*) promoter was amplified from adult zebrafish genome by polymerase chain reaction (PCR) using forward primer (5′-CCGCTCGAGCCTTCCCTTC-

https://dx.doi.org/10.1021/acssensors.9b02489
ACS Sens. 2020, 5, 823−830

TACTTTTGACGTCC-3′) containing a *Xho* I restriction site and reverse primer (5′-CCCAAGCTTGATGCCTGTGTCTTT-GAGTTGC-3′) containing a *Hind* III restriction site.[21,22] The *krt4* promoter was inserted between the *Xho* I and *Hind* III restriction sites before the sensor C3 gene (Figure 1A). Sensor C3 gene encodes a fusion protein consisting of three parts: a cyan fluorescent protein (CFP), a 16 amino acid linker containing four amino acids, DEVD, which is the cleavage site of caspase-3/7, and a yellow fluorescent protein (YFP) (Figure 2A). The details of sensor C3 can be found in our previous publication.[18] The construct also contained a poly (A) tail and two *Tol2* transposase-recognition sequences (Figure 1A). This construct was named as pSK-krt4-C3. The *Tol2* transposase mRNA was transcribed in vitro using the mMESSAGE mMACHINE SP6 Transcription Kit (Ambion).

For the microinjection, pSK-krt4-C3 (final concentration, 50 ng/μL) and the *Tol2* transposase mRNA (final concentration, 100 ng/μL) were mixed. Approximately 2−4 nL of the mixed solution was injected into one-cell stage zebrafish embryos using an MPPI-3 pressure injector from Applied Scientific Instrumentation. The fluorescence-positive embryos were screened and raised to adulthood. The adult founder zebrafish were crossed with WT zebrafish to produce the transgenic zebrafish.

Live Zebrafish Imaging. Zebrafish embryos and larvae were mounted in 1% low-melting agarose gel with 1× tricaine (0.016%) or 3% methylcellulose with 1× tricaine. The adult zebrafish were anesthetized with 1× tricaine and imaged within 5 min and put back into fresh fish water for recovery.

A Carl Zeiss LSM 710 confocal laser scanning microscope was used for the FRET imaging. A 458 nm laser was used to excite the donor molecule (CFP) of sensor C3. The emissions of 460−500 nm (CFP image, colored blue) and 520−550 nm (YFP image, colored green) were collected simultaneously by two channels using identical parameters such as the same pinhole value and gain value through a 10×, 20×, or 40× objective. The reduction in the FRET effect (YFP/CFP emission ratio) can be represented by the shift in color from green to blue in the merged FRET image. The merged green cells were considered nonapoptotic cells, and the merged blue cells were considered apoptotic cells. The *z*-stack images were processed by maximum intensity projection using ImageJ software.

Immunofluorescence. Zebrafish larvae were sacrificed with icy water and then fixed in 4% paraformaldehyde solution prepared in phosphate-buffered saline (PBS) at 4 °C for 12−16 h. For dehydration, the fixed larvae were transferred to a 30% sucrose solution prepared with PBS at 4 °C for 24−72 h. The dehydrated larvae were embedded in the Shandon Cryomatrix embedding resin (Thermo Scientific, 6769006). The larvae sections (14 μm) were prepared with a Leica CM3050S research cryostat at −20 °C. Sections were blocked with 1% bovine serum albumin (BSA) and 0.1% Triton X-100 in PBS for 1 h at room temperature and then coated with rabbit anti-green fluorescent protein (GFP) primary antibody (Cell Signaling, #2956, 1:200) overnight at 4 °C. The sections were washed with PBS and then incubated with Alexa Fluor 488-conjugated goat anti-rabbit secondary antibody (Thermo Fisher Scientific, A-11034, 1:200) for 1 h at room temperature. The sections were washed with PBS and mounted with Mowiol (Millipore, 475904) mounting medium. The sections were imaged using a Carl Zeiss LSM 710 confocal laser scanning microscope with a 488 nm laser.

Western Blotting. Zebrafish larvae (20−30) were sacrificed with icy water and then homogenized with a D1000 handheld homogenizer (Benchmark Scientific) in 200 μL of radioimmunoprecipitation assay (RIPA) buffer containing protease inhibitors on ice. Lysates were kept on ice for 30 min and then sonicated at 4 °C to release additional proteins. After sonication, the lysates were centrifuged at 13 000 rpm for 15 min at 4 °C to collect the supernatant. The protein concentration was determined by Bradford assay. Approximately 100 μg of protein was loaded in each well of a 15% sodium dodecyl sulfate-polyacrylamide gel electrophoresis (SDS-PAGE) gel. After electrophoresis, the proteins were transferred to a nitrocellulose membrane and blocked with 5% nonfat dry milk in TBST for 1 h at room temperature. The nitrocellulose membrane was then coated with rabbit anti-GFP primary antibody (Cell Signaling, #2956, 1:2500) or rabbit anti-β-actin primary antibody (Cell Signaling, #4967, 1:2500) overnight at 4 °C and HRP-conjugated goat anti-rabbit secondary antibody (Bio-Rad, #1706515, 1:5000) at room temperature for 1 h. The chemiluminescence signal was detected using a ChemiDoc MP Imaging System (Bio-Rad).

UV Irradiation of the Zebrafish. Live zebrafish larvae or adult zebrafish were exposed twice to UVC (254 nm) generated by an ultraviolet cross-linker CL-1000 (UVP) at a dosage of 200 mJ/cm^2.

Statistics. All of the results are expressed as the mean ± standard deviation (SD). Statistical tests were performed using a one-way analysis of variance (ANOVA) with Tukey's post hoc test for multiple comparisons using GraphPad Prism 7 software. A p-value <0.05 was considered to be statistically significant. The significance is indicated as $^*p < 0.05$, $^{**}p < 0.01$, $^{***}p < 0.001$, and $^{****}p < 0.0001$ in the figures.

RESULTS AND DISCUSSION

Generation and Characterization of the Sensor Zebrafish. A zebrafish skin-specific promoter, *krt4*,[21,22] was selected for driving the expression of sensor C3 in the skin of zebrafish. The DNA sequence of the *krt4* promoter was amplified from a WT zebrafish genome and placed upstream of the sensor C3 gene, which had been amplified from its original construct[18] to generate the zebrafish *Tol2* transposon construct: pSK-krt4-C3 (Figure 1A). The pSK-krt4-C3 plasmids together with the *Tol2* transposase mRNA were co-injected into one-cell stage zebrafish embryos. After micro-injection, green fluorescence-positive embryos were selected and raised to adulthood. The adult founder zebrafish were crossed with WT zebrafish to produce transgenic sensor zebrafish, which is named as Tg(*krt4*:sensor C3).

The green fluorescence of sensor C3 became obviously visible in Tg(*krt4*:sensor C3) zebrafish larvae at 12 h after fertilization (hpf) and was maintained through development (Figure 1B). Observation at higher magnification revealed a strong and uniform expression of sensor C3 in the skin cells of the zebrafish larvae at 72 hpf (Figure 1B). The skin-specific expression of sensor C3 was validated by immunofluorescence staining using an anti-GFP antibody, which can recognize both CFP and YFP since CFP and YFP are derived from GFP.[18] The results showed that sensor C3 was mainly localized in the outermost single layer of Tg(*krt4*:sensor C3) zebrafish skin cells, covering the two examined areas of the trunk/yolk sac (Figure 1B) and head (Figure S1).

Scales are used to protect adult zebrafish and there are skin cells on the top of scales.[23,24] Interestingly, the expression of sensor C3 could be observed in these skin cells located on the surface of the zebrafish scales. The expression of sensor C3 could also be observed in the skin of the caudal fin and anal fin in the adult Tg(*krt4*:sensor C3) zebrafish (Figure 1B).

In this study, we achieved the skin-specific expression of sensor C3 in zebrafish. Similarly, sensor C3 can also be driven by other tissue-specific promoters to be expressed in other tissues such as the heart, liver, and neurons. The transparency of zebrafish and the application of advanced imaging techniques such as light-sheet microscopy[13] may allow the detection of apoptosis in deeper tissues of live sensor zebrafish.

Sensor Zebrafish Can Detect Apoptosis at Single-Cell Resolution in Live Animal. According to the design and working principle of the sensor zebrafish, when sensor C3 proteins in the skin cells are excited at 458 nm, the emission energy of the CFP is transferred to excite the YFP, which emits green fluorescence at 535 nm. Thus, the live sensor cells

https://dx.doi.org/10.1021/acssensors.9b02489
ACS Sens. 2020, 5, 823−830

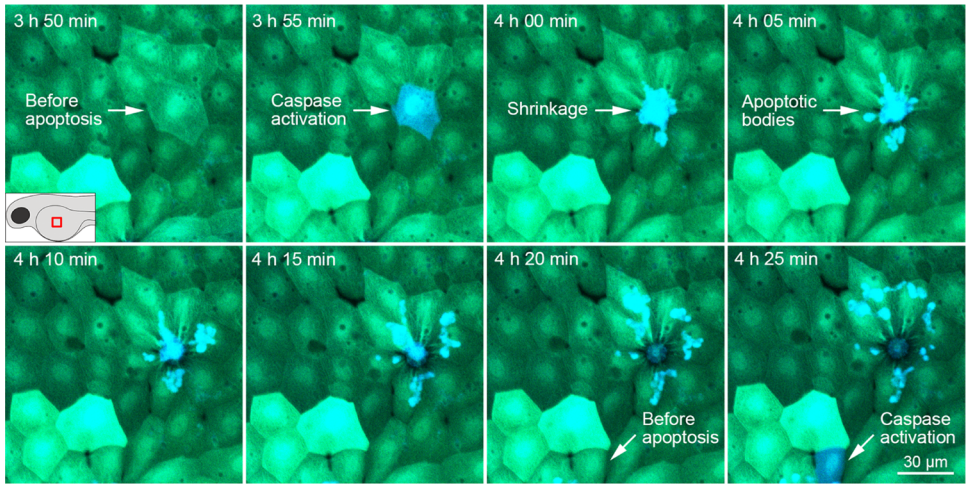

Figure 3. Real-time tracking of skin cell apoptosis in live sensor zebrafish after UV irradiation. Tg(*krt4*:sensor C3) zebrafish larvae (48 hpf) were irradiated twice with UV rays at a dosage of 200 mJ/cm^2. After UV irradiation, time-lapse FRET imaging was used to capture the rapid apoptotic process in live zebrafish. The imaging area is illustrated in the zebrafish cartoon. The time after UV irradiation is indicated in each image.

appear green in the FRET image, which is produced by merging the CFP image with the YFP image. When caspase-3/7 are activated during apoptosis, they cleave the sensor C3 proteins at the DEVD site to stop the energy transfer between the CFP and the YFP. As a result, the apoptotic sensor cells emit more blue fluorescence at 480 nm and appear in blue in the FRET image (Figure 2A).

To test whether the sensor C3 synthesized in zebrafish can produce the FRET effect, live Tg(*krt4*:sensor C3) zebrafish were excited using a 458 nm laser, and the emissions of 460−500 nm (CFP image, colored blue) and 520−550 nm (YFP image, colored green) were collected simultaneously by two channels using a Carl Zeiss LSM 710 laser scanning microscope. The automatically merged FRET image appeared in green, indicating that the zebrafish sensor cells can produce the FRET effect (Figures 2B and S2).

We then tested whether sensor C3 could detect apoptosis in the zebrafish. The Tg(*krt4*:sensor C3) zebrafish larvae were irradiated twice with UVC (254 nm) generated by an ultraviolet cross-linker CL-1000 (UVP) at a dosage of 200 mJ/cm^2. Four hours after the zebrafish were exposed to the UV irradiation, the FRET images were generated directly from the live zebrafish, and they showed that some zebrafish sensor cells appeared blue, indicating that they were undergoing apoptosis (Figures 2B and S2). The results from a *z*-stack imaging analysis showed the spatial distribution of the apoptotic cells in another Tg(*krt4*:sensor C3) sensor zebrafish larvae at 4 h (Video S1) and 8 h (Video S2) after UV irradiation.

Eight hours after UV irradiation, the control and irradiated zebrafish larvae were homogenized for Western blotting analysis. Using an anti-GFP antibody, the full-length sensor C3 proteins were detected at the expected molecular weight of 56 kD from the sensor zebrafish, but no such band was detected from the WT zebrafish. More importantly, after UV irradiation, some sensor C3 protein molecules were cleaved into two bands, which were expected to be CFP and YFP (Figure 2C).

We irradiated 3-month-old adult Tg(*krt4*:sensor C3) zebrafish with UV rays. The FRET images showed that most skin cells appeared green before UV irradiation, and some of them changed to blue 4 h after being irradiated. This result indicates that the sensor C3 expressed in adult zebrafish can also detect apoptosis (Figure 2D). This is the first report of apoptosis being detected in live adult animals.

In our previous study, we observed that the YFP/CFP emission ratio of sensor C3 could be reduced for 4−5-fold in response to caspase-3 activation and the sensor proteins could be cleaved when exposed to caspase-3 at nanomolar concentration.[18] This indicates that sensor zebrafish Tg(*krt4*:sensor C3) are very sensitive and can capture most of the caspase-3/7-dependent apoptotic skin cells. In the transgenic sensor zebrafish, the sensor C3 gene was integrated into the zebrafish genome and could be passed to offspring zebrafish by simple breeding. The stably expressed sensor proteins inside of the zebrafish cells enable the noninvasive detection of apoptosis. Another important advantage of our detection method is that the apoptotic cells can be detected using conventional confocal microscopy without postacquisition procedures. This advantage makes the sensor zebrafish user-friendly.

Sensor Zebrafish Can Capture the Fast Dynamics of Apoptosis Induced by UV Irradiation. After validating the ability of sensor zebrafish to detect apoptosis, we wanted to use the sensor zebrafish to determine the dynamic profile of apoptosis in live animals, which can be very challenging due to the dynamic and transient nature of apoptosis. To achieve this goal, the Tg(*krt4*:sensor C3) zebrafish larvae were irradiated with UV, and FRET images were taken every 5 min from the skin cells of the live zebrafish. The FRET images showed that at 3 h 50 min after UV irradiation, all the skin cells were green. However, in just 5 min, one cell changed color from green to blue, indicating caspase-3 was activated. This blue cell shrunk another 5 min later and started to form apoptotic bodies within an additional 5 min (Figure 3). Other sensor cells within the same observation field also displayed a rapid apoptotic process. For example, from 4 h 20 min to 4 h 25 min, one cell at the bottom of the panel changed color from green to blue (Figure 3). More green cells changed to blue and formed apoptotic bodies in less than 30 min (Figure S3A).

Besides apoptosis, the sensor zebrafish can also detect necrotic cell death. For example, from a time-lapse FRET imaging analysis, we observed some skin cells in Tg(*krt4*:sensor C3) zebrafish lost fluorescence without color change and completely disappeared rapidly after UV

https://dx.doi.org/10.1021/acssensors.9b02489
ACS Sens. 2020, 5, 823−830

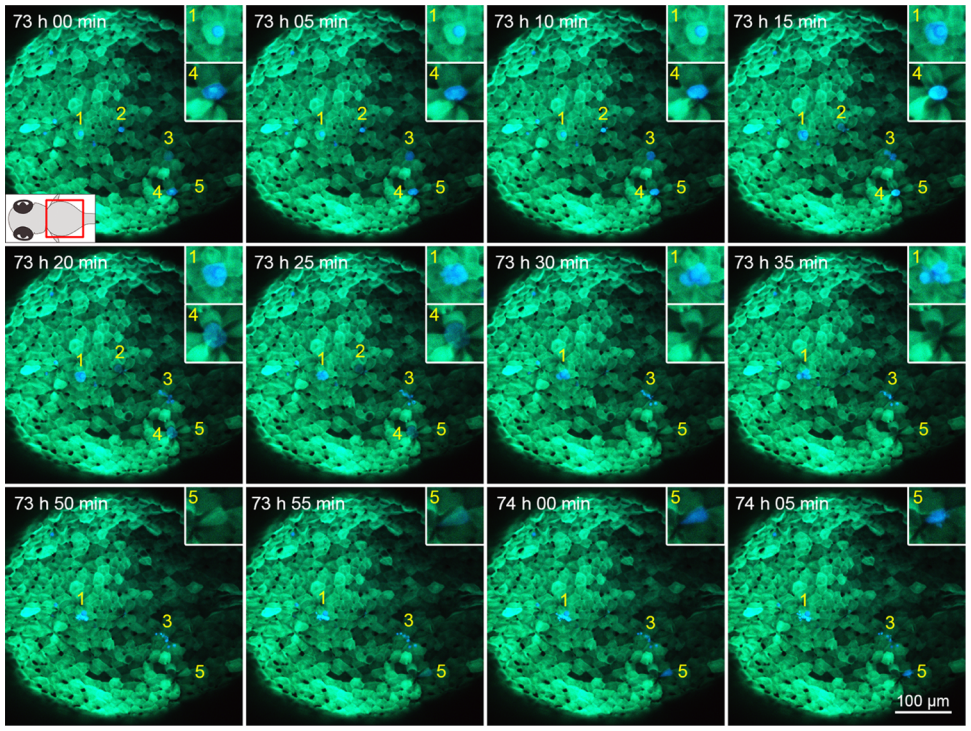

Figure 4. Real-time tracking of skin cell apoptosis in live sensor zebrafish during development. FRET imaging was used to detect cell apoptosis during the natural skin development in the yolk sac region of the Tg(*krt4*:sensor C3) zebrafish. The blue dot on top of cell 1 is an apoptotic body from another apoptotic cell. The imaging area is illustrated in the zebrafish cartoon. The time after fertilization is indicated in each image.

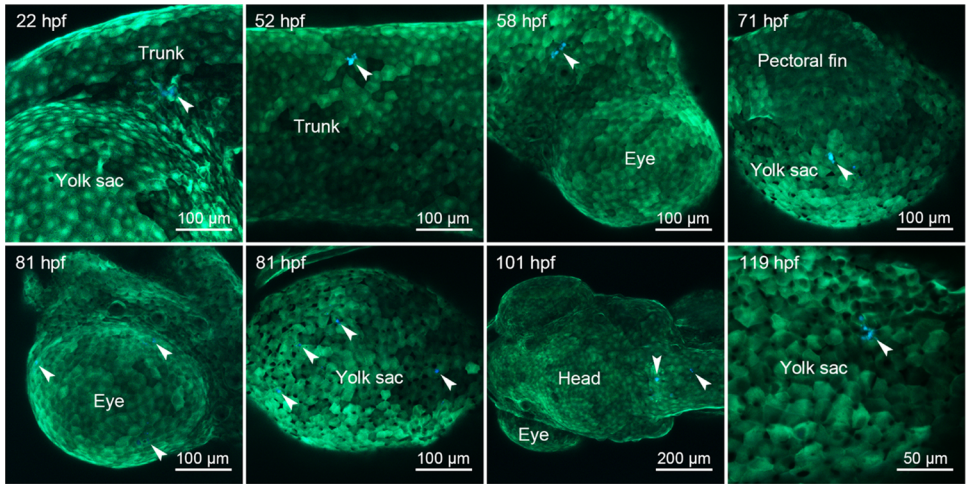

Figure 5. Spatiotemporal tracking of apoptosis in live sensor zebrafish during development. FRET imaging was used to monitor apoptosis in different parts of the skin in the same Tg(*krt4*:sensor C3) zebrafish during development. The developmental time and anatomical structures are indicated in each image. The arrowheads indicate apoptotic cells.

irradiation, indicating these cells underwent necrosis. This means that sensor C3 can distinguish live cells, apoptotic cells, and necrotic cells at the same time in live zebrafish (Figure S3B and Video S3).

During Normal Development, Zebrafish Skin Cells Can Complete the Processes of Caspase-3 Activation and Apoptosis in 30 min. In the above study, we showed that using an exogenous apoptosis inducer such as UV irradiation, caspase-3 could be activated in zebrafish skin cells in 5 min and apoptosis could be completed in 30 min. The next important question is how fast the naturally occurring apoptosis is when the skin cells receive endogenous apoptotic signal(s) during the development. To answer this important question, we performed time-lapse FRET imaging in the yolk sac region of the Tg(*krt4*:sensor C3) zebrafish during early development. Within just 1 h 35 min, we observed that 7−8 embryonic zebrafish skin cells underwent apoptosis (Figures 4, S4, and Video S4). From the five indicated cells, we observed a rapid and dynamic apoptotic process very similar to what we have observed in UV irradiation-induced apoptosis. In particular, we observed that cells 1 and 5 changed from green to blue in 5 min (73 h 10−15 min after fertilization; 73 h and 50−55 min after fertilization). After caspase-3 activation in these five cells, it took 15 min for cells 1, 3, and 5 to form apoptotic bodies, and it took approximately 30 min, for cells 2 and 4 to be engulfed by other cells.

https://dx.doi.org/10.1021/acssensors.9b02489
ACS Sens. 2020, 5, 823−830

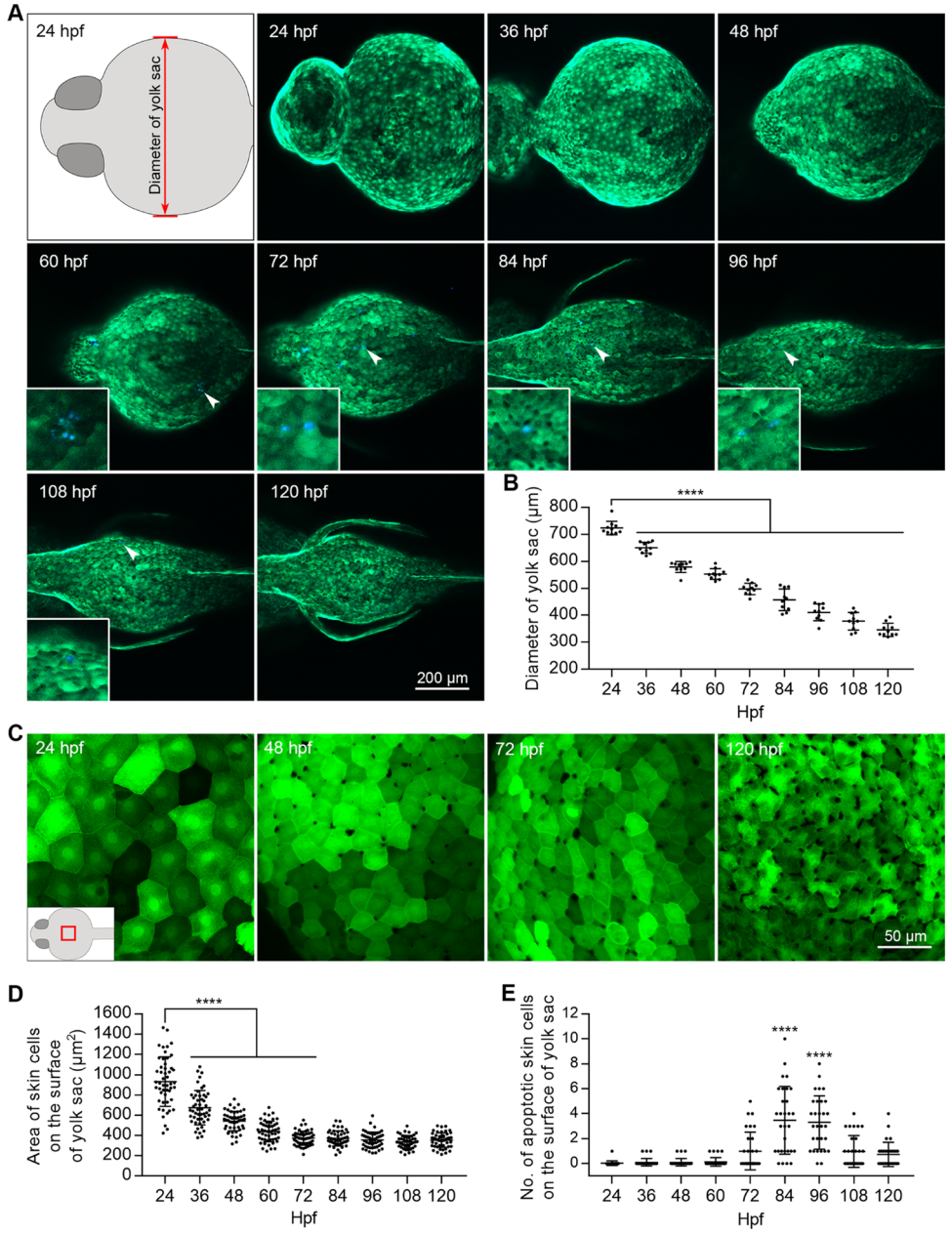

Figure 6. Zebrafish use apoptosis to remove excess skin cells during early development. (A) FRET imaging of the same Tg(*krt4*:sensor C3) zebrafish during early development. The images show morphological changes of the yolk sac and the presence of apoptotic blue cells during this period. The developmental time is indicated in each image. The arrowheads indicate apoptotic cells. An enlarged image is shown in the white box. (B) Quantified data show a gradual decrease in yolk sac diameter during development (n = 10 for each time point). (C) Fluorescence images of zebrafish yolk sac skin cells show a gradual decrease in the cell area. The imaging area is illustrated in the zebrafish cartoon. All the images were taken at the same magnification and share the same scale bar here. (D) Quantified area of the skin cells on the surface of yolk sac between 24 and 120 hpf (n = 50 for each time point). The area was measured by ImageJ software. (E) Number of apoptotic skin cells on the surface of yolk sac per zebrafish between 24 and 120 hpf (n = 30 for each time point; the zebrafish shown in (A) was not included in quantification). Statistical differences in (E) were compared between 24 hpf and other time points using one-way ANOVA with Tukey's post hoc test. ****$p < 0.0001$.

Taking all the tracking results together, we can summarize that, although UV irradiation and skin cell development use different mechanisms to induce apoptosis, both executed apoptosis rapidly by activating caspase-3 within 5 min and completing apoptosis in 30 min. Some apoptotic bodies lasted for a longer time, which may be due to the lack of phagocytotic cells in the surrounding area.

Apoptosis Can Occur in Different Parts of Sensor Zebrafish Skin throughout the Development. To determine the spatiotemporal occurrence of apoptosis during zebrafish development, we conducted FRET imaging on the same Tg(*krt4*:sensor C3) zebrafish within 120 hpf. We found that apoptosis could occur at different time points during embryonic development, such as from 22 to 119 hpf, and in different parts of zebrafish skin, including the trunk, eye, yolk sac, and head (Figure 5).

Discovering a New Role of Apoptosis in Removing Excess Skin Cells during Zebrafish Development. Zebrafish start to eat food 5 days postfertilization (dpf); therefore, within the first 5 days of zebrafish development, they

https://dx.doi.org/10.1021/acssensors.9b02489
ACS Sens. 2020, 5, 823−830

rely on internal nutrients stored in the yolk sac.[25] As a result, the size of the yolk sac is gradually reduced during this period. Specifically, we found that the average diameter of a yolk sac was reduced from 723.8 ± 25.1 μm at 24 hpf to 346.1 ± 24.6 μm at 120 hpf (Figure 6A,B).

To understand how zebrafish skin copes with the diameter reduction and shape change in the yolk sac region, we examined skin cells in this region between 24 and 120 hpf. We found that, in the region of the yolk sac, the area of skin cells quickly decreased from 932.3 ± 244.4 to 373.6 ± 68.8 μm^2 between 24 and 72 hpf but remained unchanged between 72 and 120 hpf (Figures 6C,D and S5A). We also observed that some of the skin cells underwent cell division, which may contribute to the reduction in skin cell size during early development (Figure S5B and Video S5).

As the area of skin cells was not significantly reduced between 72 and 120 hpf, we then examined whether some of the skin cells were removed by apoptosis to cope with the change of the yolk sac. FRET imaging was used to measure the number of apoptotic cells that appeared in the yolk sac region every 12 h between 24 and 120 hpf (Figure 6A). The quantified results showed that very few apoptotic cells were detected within the first 60 hpf and that the number of apoptotic cells started to increase at 72 hpf, peaked between 84 and 96 hpf, and decreased between 108 and 120 hpf (Figure 6E). These observations suggest that zebrafish may cope with the diameter reduction and shape change of the yolk sac by reducing skin cell size via division and removing excess skin cells via apoptosis.

CONCLUSIONS

We have successfully generated FRET-based sensor zebrafish, which allow noninvasive detection of apoptosis in real-time and at single-cell resolution in live zebrafish without postacquisition procedures. With these sensor zebrafish, we were able to make the following two discoveries: (1) During normal development, caspase-3 can be activated in 5 min and apoptosis can be completed in 30 min in the skin cells of live zebrafish. Such a fast dynamic of the apoptotic process was also observed in zebrafish skin cells after UV irradiation. (2) Apoptosis can occur throughout the development in different parts of zebrafish skin, with more apoptotic cells observed in the yolk sac region. This may due to the reason that zebrafish use apoptosis to remove excess skin cells to cope with the dramatic changes of the skin during yolk sac shrinkage and elongation.

In the present study, sensor C3 was driven by the *krt4* promoter to achieve the skin-specific expression of sensor C3. Similarly, sensor C3 can also be driven by other tissue-specific promoters to generate other transgenic zebrafish lines. These transgenic zebrafish lines may enable the detection of apoptosis in different organs and tissues such as the heart, liver, gonads, and neurons in live zebrafish. These transgenic zebrafish lines can potentially contribute to the study of the apoptosis involved in the development, regeneration, aging, and pathological processes.

ASSOCIATED CONTENT

Supporting Information

The Supporting Information is available free of charge at https://pubs.acs.org/doi/10.1021/acssensors.9b02489.

Expression of sensor C3 in sensor zebrafish; skin cell apoptosis after UV irradiation; real-time tracking of skin cell apoptosis after UV irradiation; real-time tracking of skin cell apoptosis during natural development; size of the skin cells decreased through cell division during development; and list of key reagents used in this study (PDF)

Spatial distribution of the apoptotic cells in Tg(*krt4*:sensor C3) sensor zebrafish larvae 4 h after UV irradiation (AVI)

Spatial distribution of the apoptotic cells in another Tg(*krt4*:sensor C3) sensor zebrafish larvae 8 h after UV irradiation (AVI)

Time-lapse imaging of apoptotic skin cells after UV irradiation (AVI)

Time-lapse imaging of apoptotic skin cells during natural development (AVI)

The division of skin cells during development (AVI)

AUTHOR INFORMATION

Corresponding Author

Kathy Qian Luo − *Faculty of Health Sciences, University of Macau, Macao SAR, China*; Email: kluo@um.edu.mo

Authors

Hao Jia − *Faculty of Health Sciences, University of Macau, Macao SAR, China*; orcid.org/0000-0003-4710-5689

Yanlong Song − *Faculty of Health Sciences, University of Macau, Macao SAR, China*

Bin Huang − *Faculty of Health Sciences, University of Macau, Macao SAR, China*

Wei Ge − *Faculty of Health Sciences, University of Macau, Macao SAR, China*

Complete contact information is available at: https://pubs.acs.org/10.1021/acssensors.9b02489

Author Contributions

K.Q.L., H.J., and W.G. conceived of the research. H.J. and K.Q.L. designed the experiments. H.J. and Y.S. constructed the sensor C3 plasmids for microinjection. H.J., Y.S., and B.H. performed the microinjection. H.J. performed other experiments. H.J. and K.Q.L. analyzed the data. H.J. and K.Q.L. prepared the manuscript.

Notes

The authors declare no competing financial interest.

ACKNOWLEDGMENTS

This work was funded by Start-Up Research Grant (SRG2016-00068-FHS) and FHS Internal Project Grant of the University of Macau.

REFERENCES

(1) Green, D. R. The Coming Decade of Cell Death Research: Five Riddles. *Cell* **2019**, *177*, 1094−1107.

(2) Hanahan, D.; Weinberg, R. A. Hallmarks of cancer: the next generation. *Cell* **2011**, *144*, 646−674.

(3) Meynier, S.; Rieux-Laucat, F. FAS and RAS related Apoptosis defects: From autoimmunity to leukemia. *Immunol. Rev.* **2019**, *287*, 50−61.

(4) Lambelet, M.; Terra, L. F.; Fukaya, M.; Meyerovich, K.; Labriola, L.; Cardozo, A. K.; Allagnat, F. Dysfunctional autophagy following exposure to pro-inflammatory cytokines contributes to pancreatic β-cell apoptosis. *Cell Death Dis.* **2018**, *9*, No. 96.

(5) Cordeiro, M. F.; Guo, L.; Coxon, K. M.; Duggan, J.; Nizari, S.; Normando, E. M.; Sensi, S. L.; Sillito, A. M.; Fitzke, F. W.; Salt, T. E.; Moss, S. E. Imaging multiple phases of neurodegeneration: a novel approach to assessing cell death in vivo. *Cell Death Dis.* **2010**, *1*, No. e3.
(6) Wang, C.; Youle, R. J. The role of mitochondria in apoptosis. *Annu. Rev. Genet.* **2009**, *43*, 95−118.
(7) Elmore, S. Apoptosis: a review of programmed cell death. *Toxicol. Pathol.* **2007**, *35*, 495−516.
(8) Takemoto, K.; Kuranaga, E.; Tonoki, A.; Nagai, T.; Miyawaki, A.; Miura, M. Local initiation of caspase activation in Drosophila salivary gland programmed cell death in vivo. *Proc. Natl. Acad. Sci. U.S.A.* **2007**, *104*, 13367−13372.
(9) Loo, D. T. In Situ Detection of Apoptosis by the TUNEL Assay: An Overview of Technique. In *DNA Damage Detection In Situ, Ex Vivo, and In Vivo*; Springer: 2011; Vol. *682*, pp 3−13.
(10) Rieger, A. M.; Nelson, K. L.; Konowalchuk, J. D.; Barreda, D. R. Modified annexin V/propidium iodide apoptosis assay for accurate assessment of cell death. *J. Visualized Exp.* **2011**, No. e2597.
(11) Bardet, P.-L.; Kolahgar, G.; Mynett, A.; Miguel-Aliaga, I.; Briscoe, J.; Meier, P.; Vincent, J.-P. A fluorescent reporter of caspase activity for live imaging. *Proc. Natl. Acad. Sci. U.S.A.* **2008**, *105*, 13901−13905.
(12) To, T.-L.; Piggott, B. J.; Makhijani, K.; Yu, D.; Jan, Y. N.; Shu, X. Rationally designed Fluorogenic protease reporter visualizes spatiotemporal dynamics of apoptosis in vivo. *Proc. Natl. Acad. Sci. U.S.A.* **2015**, *112*, 3338−3343.
(13) Keller, P. J.; Schmidt, A. D.; Wittbrodt, J.; Stelzer, E. H. Reconstruction of Zebrafish early embryonic development by scanned light sheet microscopy. *Science* **2008**, *322*, 1065−1069.
(14) van Ham, T. J.; Mapes, J.; Kokel, D.; Peterson, R. T. Live imaging of apoptotic cells in Zebrafish. *FASEB J.* **2010**, *24*, 4336−4342.
(15) Andrews, N.; Ramel, M.-C.; Kumar, S.; Alexandrov, Y.; Kelly, D. J.; Warren, S. C.; Kerry, L.; Lockwood, N.; Frolov, A.; Frankel, P.; et al. Visualising apoptosis in live Zebrafish using fluorescence lifetime imaging with optical projection tomography to map FRET biosensor activity in space and time. *J. Biophotonics* **2016**, *9*, 414−424.
(16) To, T.-L.; Schepis, A.; Ruiz-González, R.; Zhang, Q.; Yu, D.; Dong, Z.; Coughlin, S. R.; Shu, X. Rational design of a GFP-based Fluorogenic caspase reporter for imaging apoptosis in vivo. *Cell Chem. Biol.* **2016**, *23*, 875−882.
(17) Zhang, Q.; Schepis, A.; Huang, H.; Yang, J.; Ma, W.; Torra, J.; Zhang, S.-Q.; Yang, L.; Wu, H.; Nonell, S.; et al. Designing a Green Fluorogenic Protease Reporter by Flipping a Beta Strand of GFP for Imaging Apoptosis in Animals. *J. Am. Chem. Soc.* **2019**, *141*, 4526−4530.
(18) Luo, K. Q.; Yu, V. C.; Pu, Y.; Chang, D. C. Application of the fluorescence resonance energy transfer method for studying the dynamics of caspase-3 activation during UV-induced apoptosis in living HeLa cells. *Biochem. Biophys. Res. Commun.* **2001**, *283*, 1054−1060.
(19) Tian, H.; Ip, L.; Luo, H.; Chang, D. C.; Luo, K. Q. A high throughput drug screen based on fluorescence resonance energy transfer (FRET) for anticancer activity of compounds from herbal medicine. *Br. J. Pharmacol.* **2007**, *150*, 321−334.
(20) Anand, P.; Fu, A.; Teoh, S. H.; Luo, K. Q. Application of a fluorescence resonance energy transfer (FRET)-based biosensor for detection of drug-induced apoptosis in a 3D breast tumor model. *Biotechnol. Bioeng.* **2015**, *112*, 1673−1682.
(21) Gong, Z.; Ju, B.; Wang, X.; He, J.; Wan, H.; Sudha, P. M.; Yan, T. Green fluorescent protein expression in germ-line transmitted transgenic Zebrafish under a stratified epithelial promoter from Keratin8. *Dev. Dyn.* **2002**, *223*, 204−215.
(22) Chen, C.-F.; Chu, C.-Y.; Chen, T.-H.; Lee, S.-J.; Shen, C.-N.; Hsiao, C.-D. Establishment of a transgenic Zebrafish line for superficial skin ablation and functional validation of apoptosis modulators in vivo. *PLoS One* **2011**, *6*, No. e20654.
(23) Sire, J.-Y.; Akimenko, M.-A. Scale development in fish: a review, with description of sonic hedgehog (shh) expression in the Zebrafish (Danio rerio). *Int. J. Dev. Biol.* **2004**, *48*, 233−247.
(24) Chang, W.-J.; Hwang, P.-P. Development of Zebrafish epidermis. *Birth Defects Res., Part C* **2011**, *93*, 205−214.
(25) Clift, D.; Richendrfer, H.; Thorn, R. J.; Colwill, R. M.; Creton, R. High-throughput analysis of behavior in Zebrafish larvae: effects of feeding. *Zebrafish* **2014**, *11*, 455−461.

https://dx.doi.org/10.1021/acssensors.9b02489
ACS Sens. 2020, 5, 823−830